

Optoelectronic Jointly Tuned Terahertz Polarization Converter Based on Graphene-Semiconductor Hybrid Metasurfaces

Ting Zhang

School of Materials Science and Engineering, Shanghai University, Shanghai, China

Abstract: Polarization multiplexing or polarization conversion devices based on metasurfaces have been reported in various electromagnetic frequency bands, among which graphene-based electronically controlled devices and semiconductor-based optically controlled terahertz metasurfaces have unique advantages in terms of modulation depth and speed, respectively. However, both are often mutually constrained and difficult to satisfy simultaneously in a single device. In this paper, an electric-optical dual physical field modulation scheme is proposed to achieve broadband and efficient polarization transformation using metal-graphene-germanium heterostructured metasurfaces. By varying the Fermi level of graphene and the conductivity of the semiconductor, the linear polarization conversion efficiency of the device is effectively switched in a wide range of 99%-25%, and the polarization conversion characteristics are well maintained in the incident angle of 0-50 degrees. The proposed scheme provides a new idea for the design of terahertz polarization devices, which is expected to be applied to terahertz communication and imaging.

Keywords: Metasurface, Polarization conversion, Tunable

1. Introduction

Polarization is an important parameter of electromagnetic waves, and typical polarization types include linear polarization, circular polarization and elliptical polarization. From the electromagnetic field point of view, it refers to the trajectory of the electric field vibration, while from the photon point of view, it (circular polarization) can also be associated with the spin angular momentum [1,2]. Therefore, the polarization of light has been widely studied and applied in imaging, quantum optics and other fields, and polarization manipulation has become an important research content in modern optics and photonics [3-5]. Traditional optics based on bulk crystals are commonly used for polarization generation or conversion, such as polarizers and waveplates. Waveplates are devices based on the linear birefringence effect of optical crystals that use an appropriate thickness to create a phase shift between ordinary and extraordinary light and then superimpose them into a new polarization state. Such devices are bulky, require high processing accuracy, and can only use specific materials for each electromagnetic band [6]. More importantly, it is difficult for these devices to simultaneously control other optical parameters or realize flexible dynamic control while performing polarization conversion, which is not conducive to the multi-functional and integrated development of modern optical devices.

Electromagnetic metasurfaces are planar functional devices composed of artificially designed subwavelength meta-atoms [7]. After more than a decade of rapid development, they have made important progress in the fields of information optics [8, 9], quantum optics [4, 5], nonlinear optics, and terahertz photonics [10]. Metasurface-based electromagnetic functional devices are flexible in design, which is beneficial to improve integration. They not only provide new ideas for the development of novel optical devices, but also provide powerful tools for many fundamental physical studies. In particular, the metasurface also realizes optical linear birefringence and polarization conversion. Different from the material birefringence of traditional optical devices, the meta-atoms in metasurfaces utilize the shape birefringence effect, including dielectric or metal structures, to realize polarization conversion and wavefront modulation from microwave to ultraviolet wavelengths [11, 12]. The introduction of active materials can provide the possibility of tunable device design. For example, the carrier concentration of monolayer graphene can be changed by various doping methods, with a large tuning range. Semiconductors can achieve ultrafast modulation by generating high concentrations of carriers under femtosecond laser irradiation.

In this paper, a metasurface-based optical-electrical co-modulation terahertz polarization converter is proposed, the dynamic polarization conversion of dual-channel external field modulation is realized by introducing a single layer of graphene and semiconductor germanium into a reflective metal metasurface. At the same time, combining the high-speed characteristics of femtosecond laser modulation and the high-efficiency advantages of voltage bias F, the efficient switching of polarization conversion efficiency from 99% to 25% is realized. In addition, the device also exhibits high tolerance to the incident angle, exhibiting efficient polarization conversion properties in the range of 0-50 degrees.

2. Theoretical model

In the absence of an external bias magnetic field, the conductive properties of graphene in the bands below the infrared frequency are mainly produced by intraband transitions, whose equivalent conductivity can be calculated from the simplified Kubo formula [13]:

$$\sigma_g \approx \sigma_{intra} = i \frac{e^2 K_B T}{\pi h^2 (\omega + i\Gamma)} \left[\frac{E_F}{K_B T} + 2 \ln \left(\exp \left(-\frac{E_F}{K_B T} \right) + 1 \right) \right] \quad (1)$$

Where E_F is the Fermi level of graphene, T is the Kelvin temperature, and Γ is the carrier scattering rate (the inverse of the relaxation time τ). For weakly doped graphene, when both conditions $|E_F| \gg K_B T$ and $\hbar\omega \gg 2|E_F|$ are satisfied, the formula can be expressed in Drude form:

$$\sigma_g = \frac{iD}{\pi(\omega + i\Gamma)} = \frac{ie^2 E_F}{\pi h^2 (\omega + i\Gamma)} \quad (2)$$

where D is the Drude mass and the Fermi level is a function of the carrier concentration:

$$|E_F| = \hbar V_F (\pi |n|)^{1/2} \quad (3)$$

It can be seen that the Fermi level of graphene can be adjusted by doping, chemical surface modification, applied voltage, magnetic field, etc.

In addition, according to the Jones matrix theory, the incident and reflected waves of an anisotropic metasurface unit can be related by the reflection coefficient matrix,

$$\begin{pmatrix} E_x^r \\ E_y^r \end{pmatrix} = \begin{pmatrix} r_{xx} & r_{xy} \\ r_{yx} & r_{yy} \end{pmatrix} \begin{pmatrix} E_x^i \\ E_y^i \end{pmatrix} \quad (4)$$

The polarization conversion efficiency can be calculated by the following formula, taking x-polarized incidence as an example:

$$PCR = R_{yx} / (R_{yx} + R_{xx}) \quad (5)$$

where $R_{ij} = |r_{ij}|^2$ is the reflectivity of each polarization component.

3. Results and discussion

We propose a graphene-semiconductor optoelectronic co-tunable terahertz metasurface polarization converter, which functions as a tunable half-wave plate. When the linearly polarized terahertz wave in the x-direction is incident, most of the reflected wave will be converted to a line polarized wave in the y-direction, and similarly when a linearly polarized terahertz wave in the y-direction is incident, most of the reflected wave will be converted to a line polarized wave in the x-direction.

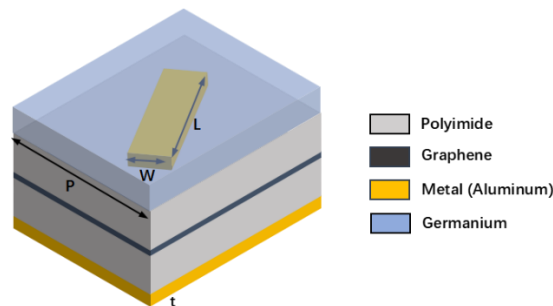


Figure 1: Schematic diagram of the unit structure.

In order to achieve the above functions, the polarization conversion unit is designed as shown in Figure 1, with a unit period is $P=68 \mu\text{m}$. Aluminum is chosen as the material for the metal rod, whose conductivity is $3.56 \times 10^7 \text{ S/m}$, the length of the metal structure is $L=82 \mu\text{m}$, the width is $W=10 \mu\text{m}$, the thickness is $t=0.2 \mu\text{m}$, and it is embedded in germanium with a thickness of $0.4 \mu\text{m}$. Polyimide with a thickness of $40 \mu\text{m}$ is used as the substrate, and silicon dioxide with a thickness of $0.2 \mu\text{m}$ is inserted in the middle of the substrate. The upper surface of the silicon dioxide is covered with a single layer of graphene, and the bottom of the overall structure is a $0.2 \mu\text{m}$ thick aluminum metal backing plate.

The simulation is performed using the frequency domain solver of the electromagnetic simulation software CST Microwave Studio, so that the incident terahertz wave is a plane linearly polarized wave, the direction of the electric field is parallel to the y-axis, and the direction of the wave vector is parallel to the z-axis. The x and y directions are set as unit cell boundary conditions, and the z directions are set as open boundaries both above and below. In the simulation process, the dielectric constant of the insulating material polyimide is set to 3.1, and the loss tangent is 0.05. The resonance properties of the structure are adjusted by setting the germanium to different values of conductivity and the graphene to different values of Fermi level and relaxation time.

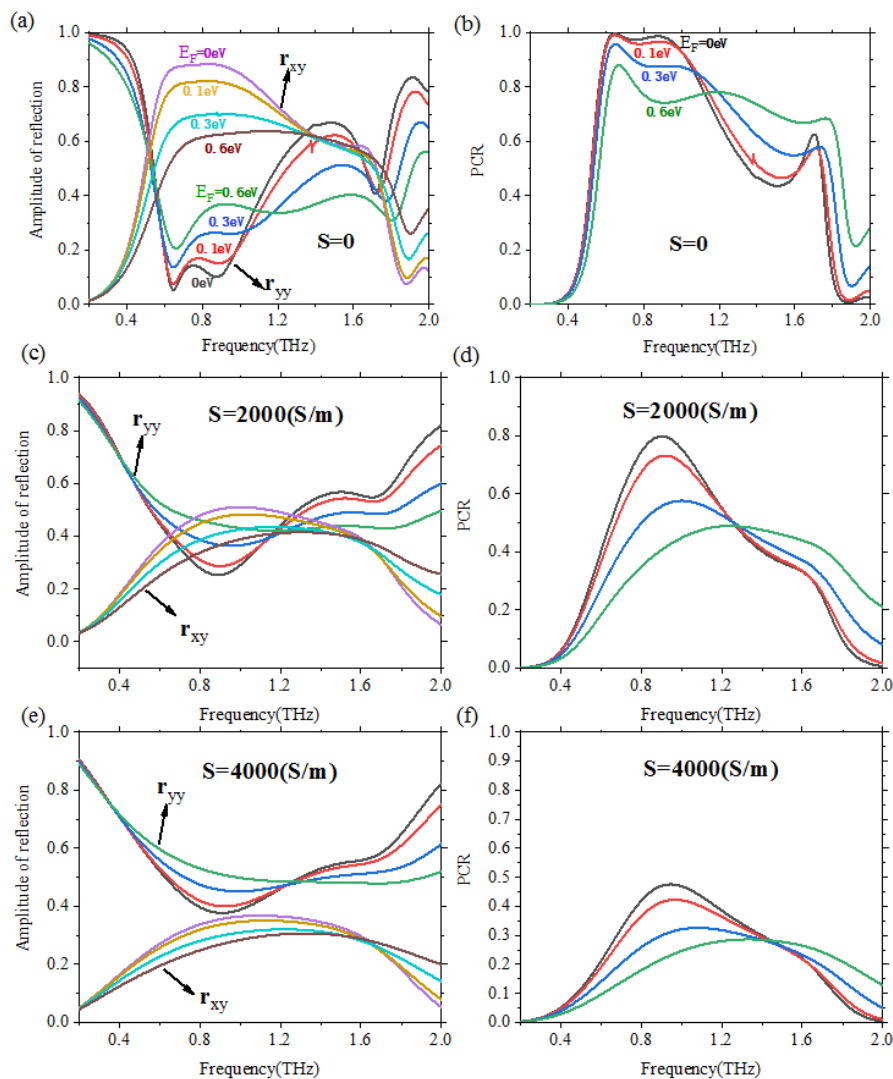


Figure 2: Combined modulation of graphene Fermi level (E_F) and germanium conductivity on polarization conversion efficiency. (a), (c), (e) reflection coefficient; (b), (d), (f) polarization Conversion efficiency.

Firstly, the joint modulation effect of graphene Fermi level (E_F) and germanium conductivity on polarization conversion properties is considered. As shown in Figure 2(a), 2(b), when the conductivity $S=0$ and Fermi level $E_F=0$, the co-polarization reflection coefficient is close to 0 near 0.8 THz, and the cross-polarization reflection is close to 1 in this frequency range, the polarization conversion efficiency

is very close to 100%, demonstrating the ability of device to rotate the polarization plane of the input linearly polarized wave by 90° with high output purity in a specific frequency range. With the gradual increase of the Fermi level, the polarization conversion efficiency decreases obviously, especially in the high frequency part. In Figure 2(c)-2(f), when the conductivity $S=2000$ (S/m), the co-polarization reflection coefficient increases sharply, the cross-polarization reflection coefficient decreases sharply, and the maximum polarization conversion efficiency is only 80%. When the conductivity $S=4000$ (S/m), the co-polarization reflection coefficient is already greater than the cross-polarization reflection coefficient, and the maximum polarization conversion efficiency is 50%. It can also be noted that at the above three conductivities, the larger the Fermi level, the larger the peak co-polarization reflectivity, the smaller the peak cross-polarization reflectivity, and the lower the peak polarization conversion efficiency.

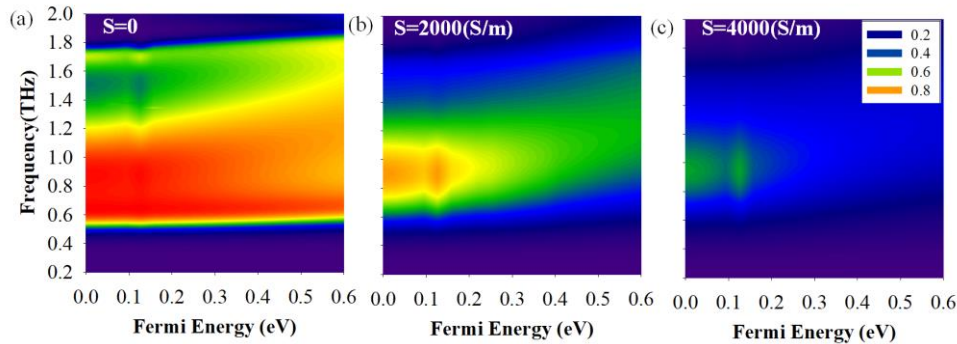


Figure 3: The joint modulation effect of graphene and germanium on polarization conversion efficiency.

In order to further observe the joint modulation effect of graphene and germanium on the polarization conversion efficiency, we carried out more detailed calculations of PCR values under different Fermi levels and germanium conductivity values, and the results are shown in Figure 3. We set the conductivities to 0, 2000 S/m, and 4000 S/m, and then took the Fermi level from 0 to 0.6 eV. It can be seen from the figure that the optoelectronic joint modulation method can effectively adjust the polarization conversion efficiency peak and bandwidth of the device.

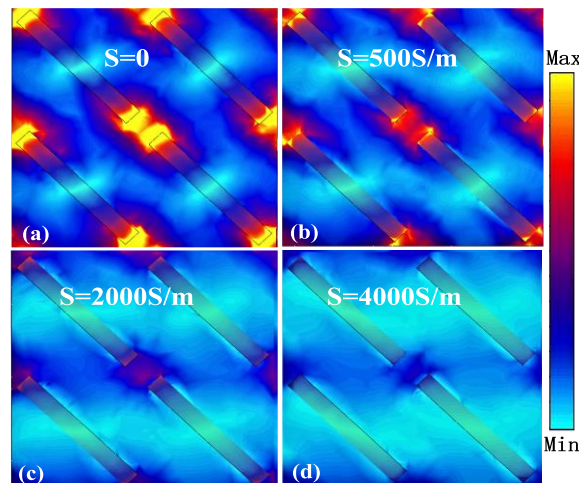


Figure 4: Electric field distribution for different germanium conductivity values.

We present the electric field distribution near rectangular metal strips for different conductivities in Figure 4. According to the simulation results in the figure, it can be concluded that the change of the conductivity of germanium has a great influence on the polarization conversion. In the process of increasing the conductivity of germanium, it changes from dielectric to metallic, so that the metal rods tend to be connected to each other, resulting in an insignificant array of metal cutting lines. On the one hand, the bipolar oscillation excited by the incident wave along the cutting line is relatively weakened, and on the other hand, it affects the polarization coupling in the multi-reflection process.

The results show a weakened cross-polarized reflection and an enhanced co-polarized reflection. In addition, when the Fermi level of graphene increases, the electrical conductivity near the insulating layer increases, which changes the coupling between the upper metal and the underlying metal backplane,

which in turn also weakens the polarization conversion capability of the device.

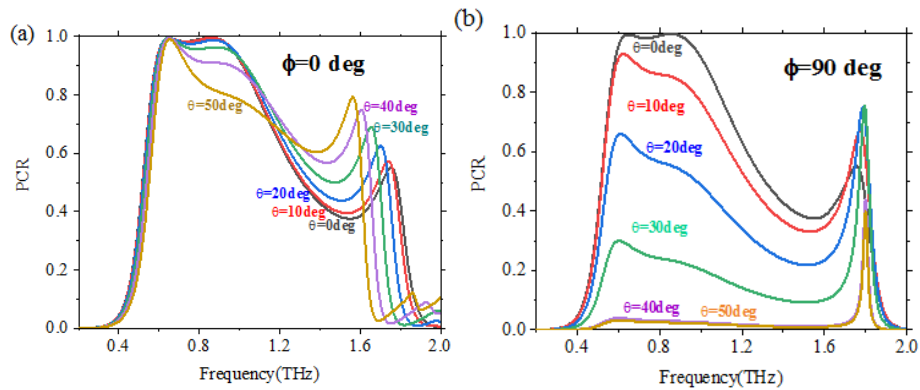


Figure 5: Polarization conversion efficiency at different angles of incidence.

Finally, in order to characterize the influence of the incident angle on the polarization conversion performance of the device, we calculated the polarization conversion efficiency for different incident angles. Figure 5 shows the polarization conversion efficiency obtained by varying the incident angle in the xoz and yoz planes. It can be found that when $\phi = 0$ degrees and changing θ , the PCR is almost unchanged in the frequency range from 0 to 0.7 THz as θ increases, and the curves overlap. After more than 0.7 THz, the PCR peak and response bandwidth have a decreasing trend. When $\phi = 90$ degrees and changing θ , with the increase of θ , the overall PCR shows a relatively large decrease. When $\theta = 40$ degrees, PCR is close to 0. This means that the different incident angles have a great influence on the polarization conversion. Generally speaking, the polarization conversion efficiency is the largest and the bandwidth is the widest at vertical incidence. The larger the incident wave deviates from the vertical incidence angle, the lower the polarization conversion efficiency.

4. Conclusion

In conclusion, this paper proposes a metasurface polarization converter with joint electro-optical dual physical field modulation. The metal-graphene-germanium hybrid structure combines the advantages of both optical and electrical control to achieve broadband and high-efficiency tunable terahertz linear polarization conversion. The modulation effect of graphene Fermi level and germanium conductivity on polarization conversion efficiency, the physical mechanism of dynamic modulation and the sensitivity of the device to the incident angle are investigated. The proposal of this scheme facilitates the further development of tunable metasurfaces and terahertz polarization devices.

References

- [1] M. Onoda, S. Murakami, and N. Nagaosa, "Hall effect of light," *Phys. Rev. Lett.* 93, 083901 (2004).
- [2] O. Hosten and P. Kwiat, "Observation of the spin Hall effect of light via weak measurements," *Science* 319, 787–790 (2008).
- [3] W. Groner, J. W. Winkelman, A. G. Harris, C. Ince, G. J. Bouma, K. Messmer, and R. G. Nadeau, "Orthogonal polarization spectral imaging: a new method for study of the microcirculation," *Nat. Med.* 5, 1209–1212 (1999).
- [4] T. Stav, A. Faerman, E. Maguid, D. Oren, V. Kleiner, E. Hasman, and M. Segev, "Quantum entanglement of the spin and orbital angular momentum of photons using metamaterials," *Science* 361, 1101–1104 (2018).
- [5] R. C. Devlin, A. Ambrosio, N. A. Rubin, J. P. B. Mueller, and F. Capasso, "Arbitrary spin-to-orbital angular momentum conversion of light," *Science* 358, 896–901 (2017).
- [6] D. Goldstein, *Polarized Light*, 3rd ed. (CRC Press, 2010)
- [7] N. Yu and F. Capasso, "Flat optics with designer metasurfaces," *Nat. Mater.* 13, 139–150 (2014).
- [8] F. Zangeneh-Nejad, D. L. Sounas, A. Alù, and R. Fleury, "Analogue computing with metamaterials," *Nat. Rev. Mater.* 6, 207–225 (2021).
- [9] Y. Zhou, H. Zheng, I. I. Kravchenko, and J. Valentine, "Flat optics for image differentiation," *Nat. Photonics* 14, 1–2 (2020).

- [10] G. Li, S. Zhang, and T. Zentgraf, "Nonlinear photonic metasurfaces," *Nat. Rev. Mater.* 2, 17010 (2017).
- [11] S. Wang, Z. Deng, Y. Wang, Q. Zhou, X. Wang, Y. Cao, B. Guan, S. Xiao, and X. Li, "Arbitrary polarization conversion dichroism metasurfaces for all-in-one full Poincaré sphere polarizers," *Light Sci. Appl.* 10, 24 (2021).
- [12] Q. Fan, M. Liu, C. Zhang, W. Zhu, Y. Wang, P. Lin, F. Yan, L. Chen, H. J. Lezec, Y. Lu, A. Agrawal, and T. Xu, "Independent amplitude control of arbitrary orthogonal states of polarization via dielectric metasurfaces," *Phys. Rev. Lett.* 125, 267402 (2020).
- [13] Y. Malevich, M. S. Ergoktas, G. Bakan, P. Steiner, and C. Kocabas, "Video-Speed Graphene Modulator Arrays for Terahertz Imaging Applications," *ACS Photonics* 7(9), 2374-2380 (2020).